Effects of the bending resonance of the floors on the vertical vibrations of buildings

Céline Chesnais, Claude Boutin, Stéphane Hans

▶ **To cite this version:**

Céline Chesnais, Claude Boutin, Stéphane Hans. Effects of the bending resonance of the floors on the vertical vibrations of buildings. 15th World conference on earthquake engineering, Sep 2012, Portugal. 10p. hal-00854963

HAL Id: hal-00854963
https://hal.science/hal-00854963

Submitted on 28 Aug 2013

HAL is a multi-disciplinary open access archive for the deposit and dissemination of scientific research documents, whether they are published or not. The documents may come from teaching and research institutions in France or abroad, or from public or private research centers.

L'archive ouverte pluridisciplinaire **HAL**, est destinée au dépôt et à la diffusion de documents scientifiques de niveau recherche, publiés ou non, émanant des établissements d'enseignement et de recherche français ou étrangers, des laboratoires publics ou privés.

Effects of the bending resonance of the floors on the vertical vibrations of buildings

C. Chesnais
IFSTTAR, Université Paris-Est, Paris, France

C. Boutin & S. Hans
DGCB, FRE CNRS 3237, ENTPE, Université de Lyon, Vaulx-en-Velin, France

SUMMARY:
Buildings are made up of beams and plates which are much stiffer in tension-compression than in bending. Thus, the vertical modes of a building (governed by the tension-compression of the walls at the macroscopic scale) can appear in the same frequency range as the bending modes of the floors. In the absence of bending resonance, the vertical vibrations are described at the macroscopic scale by the usual equation for beams in tension-compression. When there is resonance, the form of the equation is unchanged but the real mass of the structure is replaced by an effective mass which depends on the frequency. This induces abnormal response in the neighbourhood of the natural frequencies of the floors. By considering idealized buildings made up of the periodic repetition of frames, this phenomenon is evidenced theoretically thanks to the homogenization method of periodic discrete media and numerically.

Keywords: Atypical dynamics, continuous modelling, local resonance

1. INTRODUCTION

Structures with attached resonators are known to exhibit atypical dynamic behaviours. In particular, the vibrations of the main structure are reduced close to the resonance frequencies of the attachments due to energy exchange. An application of this phenomenon is the use of tuned mass dampers in buildings to mitigate wind and earthquake effects. Another example is given by a class of composite materials called metamaterials. Their main feature is the existence of a high rigidity contrast between the constituents (Auriault and Bonnet, 1985). As a result, the softer components act as distributed resonators which can completely block mechanical waves of certain frequencies (Liu, et al., 2000). At the macroscopic scale, metamaterials have effective properties which depend on the frequency. This applies to the mass leading to the generalization of the Newtonian mechanics (Milton and Willis, 2007).

In this paper, we show that buildings can behave as metamaterials. In fact, they are made up of beams and plates which present a high contrast between the tension-compression and bending rigidities. Therefore, the bending modes of the floors can appear in the same frequency range as the vertical modes of the building which are governed by the tension-compression of the walls at the global scale. The consequences of the resonance of the floors are investigated by considering periodic frame structures representing idealised buildings. A macroscopic description of the vertical dynamics is obtained thanks to the homogenization method of periodic discrete media (HPDM). This method, elaborated by Caillerie, Trompette and Verna (1989), has been extended to situations with local resonance. Its main advantage is that the macroscopic behaviour is derived rigorously from the properties of the basic frame. Moreover the analytic formulation enables to understand the role of each parameter. This method has already given interesting results on the horizontal dynamics of frame structures and buildings (Hans and Boutin, 2008; Chesnais, Boutin and Hans, 2011; Hans et al., 2012).

The principles of the HPDM method and the studied structures are described in section 2. Section 3

presents the two possible macroscopic behaviours: without and with local resonance. In section 4, emphasis is put on the consequences of the local resonance on the modal analysis and the transfer function of the structure. The results are confirmed by finite element simulations.

2. STUDIED STRUCTURES AND OVERVIEW OF THE HPDM METHOD

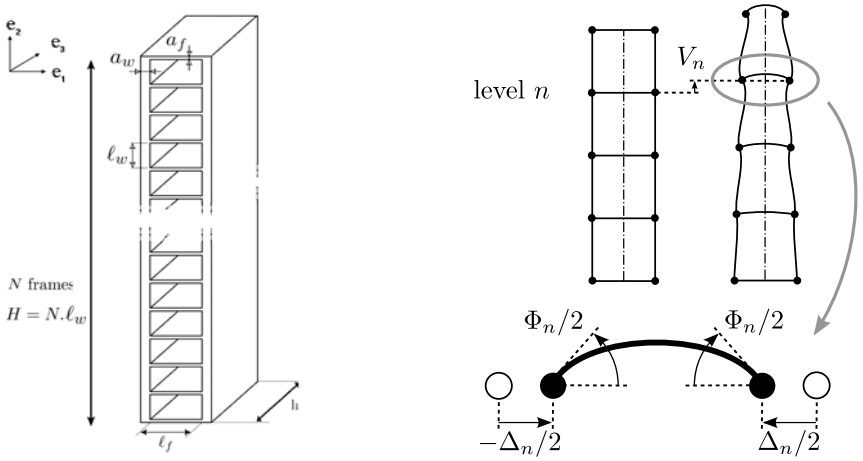

Figure 2.1. Left: class of studied structures, right: vertical kinematics

The studied structures are constituted by a pile of a large number N of identical unbraced frames called cells and made of a floor supported by two walls (see Fig. 2.1.). The walls and the floors are plates which behave as Euler-Bernoulli beams in out-of-plane motion. The parameters of floors ($i = f$) and walls ($i = w$) are: length ℓ_i, thickness a_i, cross-section area A_i, second moment of area $I_i = a_i^3 h/12$ in direction $\mathbf{e_3}$, density ρ_i, elastic modulus E_i, Poisson ratio ν_i. As the connections are assumed perfectly rigid, the motions of each endpoint connected to the same node are identical and define the discrete nodal kinematic variables of the system.

The analysis of such a periodic lattice of interconnected beams with the homogenization method of periodic discrete media (HPDM) is performed in two steps (Tollenaere and Caillerie, 1998): first, the discretisation of the balance of the structure under harmonic vibrations; second, the homogenization, leading to a continuous model elaborated from the discrete description. As the studied structures are symmetric, a change of variables is added to uncouple the horizontal and vertical kinematics. An outline of this method is given hereafter with an emphasis on its adaptation to situations with local resonance.

The discretisation consists in integrating the dynamic balance (in harmonic regime) of the beams, the unknown displacements and rotations at their extremities being taken as boundary conditions. Forces applied by an element on its extremities are then expressed as functions of the nodal kinematic variables. The balance of each element being satisfied, it remains to express the balance of forces applied to the nodes. Thus, the balance of the whole structure is rigorously reduced to the balance of the nodes.

The kinematics is characterized at any level n by the motions of the two nodes in the plane ($\mathbf{e_1}$, $\mathbf{e_2}$), i.e., the displacements in the two directions and the rotation (u_1, u_2, θ). These six variables can be replaced by (see Fig. 2.1.):

- Three variables associated to the rigid body motion of the level n: the mean displacements, $U(n)$ along $\mathbf{e_1}$ and $V(n)$ along $\mathbf{e_2}$, and the global rotation $\alpha(n)$ (differential vertical nodal motion divided by ℓ_f),
- Three variables corresponding to its deformation: the mean and differential rotations of the nodes, $\theta(n)$ and $\Phi(n)$, and the transverse dilatation $\Delta(n)$.

As mentioned before, the horizontal and vertical kinematics, respectively governed by (U, α, θ) and (V, Φ, Δ), are uncoupled. This paper focuses on the vertical vibrations. The study of the horizontal vibrations can be found in (Boutin and Hans, 2003; Hans and Boutin, 2008; Chesnais, Boutin and Hans, 2011).

Then the principles of homogenization are used to derive the differential equation describing the behaviour of the equivalent beam. The key assumption is that the cell size in the direction of periodicity ℓ_w is small compared to the characteristic size L of the vibrations of the structure. Thus, the scale ratio is small: $\varepsilon = \ell_w/L << 1$. The condition of scale separation implies that the method is limited to the first modes of vibration which have wavelengths that are much larger than the cell size. The existence of a macroscopic scale is expressed by means of macroscopic space variable x. The unknowns are continuous functions of x coinciding with the discrete variables at any level, e.g. $V_\varepsilon(x = x_n) = V(\text{level } n)$. These quantities, assumed to converge when ε approaches zero, are expanded in powers of ε: $V_\varepsilon(x) = V^0(x) + \varepsilon\ V^1(x) + \varepsilon^2\ V^2(x) + ...$ Similarly, all other unknowns, including the modal frequency, are expanded in powers of ε. As $\ell_w = \varepsilon.L$ is a small increment with respect to x, the variations of the variables between neighbouring nodes are expressed using Taylor's series; this in turn introduces the macroscopic derivatives.

To account properly for the local physics, the geometrical and mechanical characteristics of the elements are scaled according to the powers of ε. As for the modal frequency, scaling is imposed by the balance of elastic and inertia forces at the macroscopic level. This scaling insures that each mechanical effect appears at the same order whatever the ε value is. Therefore, the same physics is kept when ε approaches zero, i.e. for the homogenized model. Finally, the expansions in ε powers are introduced in the nodal balances. Those relations, valid for any small ε, lead for each ε-order to balance equations which describe the macroscopic behaviour.

In general the scale separation requires wavelengths of the compression and bending vibrations generated in each local element to be much longer than the element length at the modal frequency of the global system. In that case the nodal forces can be expanded in Taylor's series with respect to ε. This situation corresponds to a quasi-static state at the local scale. Nevertheless, at higher frequencies, it may occur that only the compression wavelength is much longer than the length of the elements while local resonance in bending appears. The expansion of the shear force and the bending moment is no longer possible. However, the homogenization remains possible through the expansion of the compression forces and leads to atypical descriptions with inner dynamics. Above this frequency range, the local resonance in both compression and bending makes impossible the homogenization process.

3. VERTICAL VIBRATIONS

3.1. Quasi-static state at the local scale

We first illustrate the classical homogenization by considering a structure as in Fig. 2.1. with thick enough elements to have a quasi-static state at the local scale. The walls and the floors are made of the same material. Their geometrical characteristics and the order of magnitude of the circular frequency ω corresponding to the vertical vibrations are given below.

$$\frac{a_w}{\ell_w} = O(\sqrt{\varepsilon}) \quad ; \quad \frac{a_f}{\ell_w} = O(\sqrt{\varepsilon}) \quad ; \quad \frac{\ell_w}{\ell_f} = O(1) \quad ; \quad \omega = O\left(\frac{1}{L}\sqrt{\frac{E_w}{\rho_w}}\right) \tag{3.1}$$

In that case, the leading order equations obtained by homogenization are:

$$\Lambda\ \omega_0^2\ V^0\ +\ 2\ E_w\ A_w\ V^{0//}\ =\ 0 \tag{3.2a}$$

$$(K_f + 3K_w)\Phi^0 - \Lambda_f\ \ell_f\ \omega_0^2\ V^0 = 0 \tag{3.2b}$$

$$\frac{12\,E_f A_f}{\ell_w\,\ell_f}\Delta^3 + 3K_w\,\Phi^{0/} = 0 \tag{3.2c}$$

$$\text{with} \quad \begin{cases} \Lambda = \Lambda_w + \Lambda_f \quad ; \quad \Lambda_w = 2\,\rho_w A_w \quad ; \quad \Lambda_f = \rho_f A_f \ell_f / \ell_w \\ K_w = 24\dfrac{E_w I_w}{\ell_w^2} \quad ; \quad K_f = 12\dfrac{E_f I_f}{\ell_w \ell_f} \end{cases} \tag{3.2d}$$

Eqn. 3.2a expresses the balance of vertical forces while Eqn. 3.2b and 3.2c come from the balance of differential moments and of differential horizontal forces. The macroscopic behaviour is given by Eqn 3.2a which corresponds to the classical description of a beam in tension-compression with the compression modulus of the two walls $2\,E_wA_w$ and the linear density Λ. Once the mean vertical displacement V is known, the "hidden" variables Φ and Δ are determined thanks to Eqn. 3.2b and 3.2c which describe the inner equilibrium of the cell. Note that Φ and Δ depend on the rigidity of the elements in bending K_w and K_f.

A systematic study in which the properties of the elements vary shows that the longitudinal vibrations with a quasi-static state at the local scale are always described by Eqn. 3.2a (Boutin and Hans, 2003).

3.2. Local resonance

To investigate the effects of the bending resonance of the floors, we now consider a structure with floors thinner than walls.

$$\frac{a_w}{\ell_w} = O(\sqrt{\varepsilon}) \quad ; \quad \frac{a_f}{\ell_w} = O(\varepsilon) \quad ; \quad \frac{\ell_w}{\ell_f} = O(1) \quad ; \quad \omega = O\left(\frac{1}{L}\sqrt{\frac{E_w}{\rho_w}}\right) \tag{3.3}$$

As the order of magnitude of a_w / a_f is not a whole power of ε, the unknowns should now be expanded in powers of $\varepsilon^{1/2}$. Moreover, because of the local resonance, the shear force and the bending moment in the floors cannot be expanded in Taylor's series. Then the homogenization provides the following equations for the first two significant orders of the balance of vertical forces. The main difference with section 3.1. is the multiplication of Λ_f by a function f depending on the frequency.

$$\Lambda_w\,\omega_0^2\,V^0 + 2\,E_w A_w\,V^{0//} = 0 \tag{3.4a}$$

$$\Lambda_w\,\omega_0^2\,V^{1/2} + 2\,E_w A_w\,V^{1/2//} + 2\,\Lambda_w\,\omega_0\,\omega_{1/2}\,V^0 + \Lambda_f\,f(\omega_0)\,\omega_0^2\,V^0 = 0 \tag{3.4b}$$

Because of the thickness contrast between the walls and the floors, Λ_f is negligible compared to Λ_w. This is the reason why we obtain a degenerate equation at the leading order. At most of the frequencies $f(\omega_0) = O(1)$ and Eqn. 3.4a is sufficient for the description of the macroscopic behaviour. However, we will see that $f(\omega_0)$ can become infinite. In that case, the inertial term related to the floors is no longer negligible. To build a macroscopic description valid for the whole frequency range of the vertical vibrations we take $\underline{V} = V^0 + \varepsilon^{1/2}\,V^{1/2}$, $\underline{\omega} = \omega_0 + \varepsilon^{1/2}\,\omega_{1/2}$ and we sum the Eqn. 3.4.

$$\Lambda(\underline{\omega})\,\underline{\omega}^2\,\underline{V} + 2\,E_w A_w\,\underline{V}^{//} = o\left(\sqrt{\varepsilon}\right) \tag{3.5a}$$

$$\text{with} \quad \begin{cases} \Lambda(\underline{\omega}) = \Lambda_w + \Lambda_f \, f(\underline{\omega}) \\ f(\underline{\omega}) = \dfrac{8}{3\pi \sqrt{\dfrac{\underline{\omega}}{\omega_{f1}}} \left[\coth\left(\dfrac{3\pi}{4} \sqrt{\dfrac{\underline{\omega}}{\omega_{f1}}} \right) + \cot\left(\dfrac{3\pi}{4} \sqrt{\dfrac{\underline{\omega}}{\omega_{f1}}} \right) \right]} \end{cases} \tag{3.5b}$$

Eqn. 3.5a looks like Eqn. 3.2a but differs fundamentally by the effective mass $\Lambda(\underline{\omega})$ which depends on the frequency. The HPDM method provides an analytical expression of the function f. Its variations according to the frequency are plotted in Fig. 3.1. It shows that $f(\underline{\omega}) \to 1$ when $\underline{\omega} \to 0$ as expected and that $|f(\underline{\omega})| \to +\infty$ when $\underline{\omega} \to \omega_{f(2k-1)}$ where $\omega_{f(2k-1)}$ are the circular frequencies of the odd normal modes of the floors with two fixed ends in bending. At most of the circular frequencies higher than ω_{f1}, we have $f(\underline{\omega}) < 1$, which means that the structure seems lighter thanks to the local resonance. Note also that $f(\underline{\omega})$ can be negative.

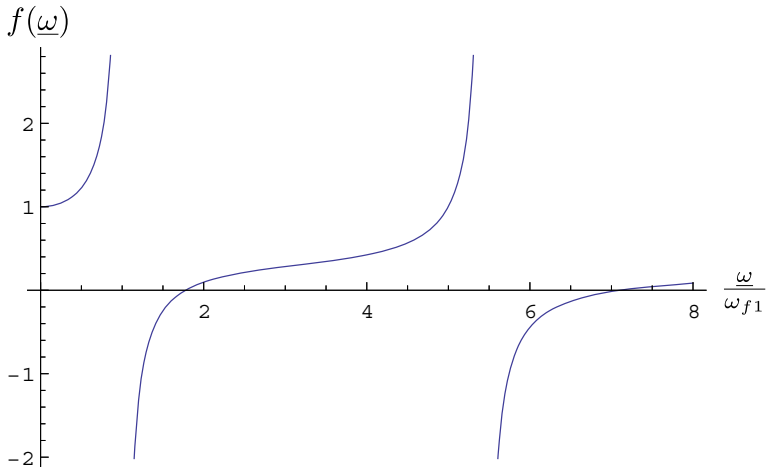

Figure 3.1. Variations of the function f according to the nondimensional frequency $\underline{\omega}/\omega_{f1}$. As the resonance frequencies of the Euler-Bernoulli beams are proportional to the sequence of the squares of the odd integers, the modes of the floors correspond to the following abscissas: $\omega_{f1}/\omega_{f1} = 3^2/3^2 = 1$, $\omega_{f2}/\omega_{f1} = 5^2/3^2 \approx 2.78$, $\omega_{f3}/\omega_{f1} = 7^2/3^2 \approx 5.44$, etc.

The effective mass differs so much from the real mass because the points of the cell are in relative motion. According to the definition of the macroscopic variables, $\underline{V}$ describes the mean vertical displacement of the nodes. At low frequencies, the whole cell undergoes the same translational motion. Consequently, the sum of inertia forces acting on the whole frame equals the real mass of the frame multiplied by the acceleration of the nodes. When bending resonance occurs, the motion of the points of the floors can strongly differ from the one of the nodes and some points can even be in antiphase. In these conditions, the sum of inertia forces acting on the basic frame is modified.

This analysis of the physical origin of the effective mass is confirmed by the consistency between the deformation of the floors and the variations of the function f. As $\underline{\omega}$ approaches ω_{f1}, the deflection is getting larger and larger because of the resonance. It is in-phase with the nodes when $\underline{\omega}$ is below ω_{f1} and in antiphase when $\underline{\omega}$ is above ω_{f1}. At the frequency of the second bending mode ω_{f2}, the in-phase motion of the two walls does not cause the resonance of the floors. Nevertheless, the motion is not uniform, which induces an effective mass smaller than the real mass.

The previous study focuses on the macroscopic description but the inner equilibrium of the cell is also affected by the local resonance. These equations contain inertial terms and they depend on the rigidity in bending of the elements. For the floors, the effective mass and the effective rigidity become infinite for the frequencies of the odd bending modes. If the walls are in resonance, their effective mass

becomes infinite for the frequencies of the odd bending modes but the rigidity becomes infinite for the frequencies of the even bending modes. The modes of the whole cell can also be excited. In the neighbourhood of all these frequencies, the structure is likely to behave atypically.

4. SOME CONSEQUENCES OF THE LOCAL RESONANCE

This section presents the consequences of the local resonance and the variations of the effective mass on the dynamic behaviour of a given structure by considering two problems frequently encountered in engineering: the modal analysis and the response to an imposed harmonic motion at the bottom. In the latter case, damping is introduced. The studied structure has been specially designed to highlight the effects of the local resonance. It is a frame structure as in Fig. 2.1. with $N = 15$ levels. The walls and the floors have the same length $\ell_w = \ell_f = 3$ m and the thickness to length ratios correspond to the orders of magnitude of section 3.2. Boutin and Hans (2003) have shown that, for the first macroscopic mode of a structure, the scale ratio can be estimated by $\varepsilon \approx \pi / (2N)$. The walls are made of concrete but the density of the floors is increased in order to have $\Lambda_f \approx \Lambda_w$ and to increase the influence of their resonance. The chosen characteristics are summarized in Eqn. 4.1.

$$\ell_w = \ell_f = 3m \quad , \quad a_w = 0.971m \quad , \quad a_f = 0.314m \quad , \quad h_w = h_f = 1m \tag{4.1}$$
$$E_w = E_f = 30000MPa \quad , \quad \nu_w = \nu_f = 0{,}2 \quad , \quad \rho_w = 2300kg/m^3 \quad , \quad \rho_f = 14225kg/m^3$$

The resonance frequencies of the floors are $f_{f1} = 52.08$ Hz, $f_{f2} = 143.56$ Hz, $f_{f3} = 281.44$ Hz.

4.1. Modal analysis

For a structure fixed at the bottom and free at the top, the solution of Eqn. 3.5a is written below.

$$\underline{V}(x) = B\sin(\alpha x) \quad \text{with} \quad \alpha^2 = \frac{\Lambda(\underline{\omega})\,\underline{\omega}^2}{2E_w A_w} \quad \text{and} \quad \cos(\alpha H) = 0 \tag{4.2}$$

Thus the resonance frequencies are given by Eqn. 4.3.

$$\alpha_k H = \frac{(2k-1)\pi}{2} \quad \Rightarrow \quad \frac{\Lambda(\underline{\omega})\,\underline{\omega}^2}{2E_w A_w} \times \left(\frac{2H}{\pi}\right)^2 = (2k-1)^2 \tag{4.3}$$

In the absence of local resonance, the effective mass is constant and there is only one solution $\underline{\omega}_k$ for each value of k. For the considered structure, this approach leads to the frequencies given in the second column of Tab. 4.1. As these frequencies are in the same range as the resonance frequencies of the floors, we cannot neglect the variations of the effective mass. Then Fig. 4.1. shows that it has two important consequences. First, the values of the resonance frequencies of the structure are modified. Second, there are several solutions $\underline{\omega}$ for each value of k. This means that the structure has the same macroscopic modal shape for several frequencies. However, at the local scale, the deformation of the floors is different. Note also that, because of the great variations of the effective mass in the neighbourhood of the odd natural frequencies of the floors, there is a solution close to these frequencies for each value of k. Consequently there is a large number of modes in a small frequency range. Just after the resonance of the floors, the effective mass is negative and there is a frequency range with no vertical modes. Usually the condition of scale separation limits homogenization to low frequencies. Since several modes of the studied structure can have the same wavelength, some high frequency modes can be correctly described by homogenization. Here, the scale ratio ε does not monotonically increase with the frequency and there is an alternation of frequencies at which homogenization applies and frequencies at which homogenization does not apply.

All these results are confirmed numerically with the finite element code CESAR-LCPC. The modes are determined for two structures. For the first one, the elements behave as Euler-Bernoulli beams as in the HPDM method. For the second one, the elements behave as Timoshenko beams which is more realistic for the chosen thickness. The resonance frequencies calculated with the finite element method and Eqn. 4.3. are given in Tab. 4.1. There is an excellent agreement between the two approaches. The use of Timoshenko beams slightly modifies the frequencies but the modal shapes are identical. The modal shapes are presented in Fig. 4.2. and they are compared with Eqn. 4.2. in Fig. 4.3.

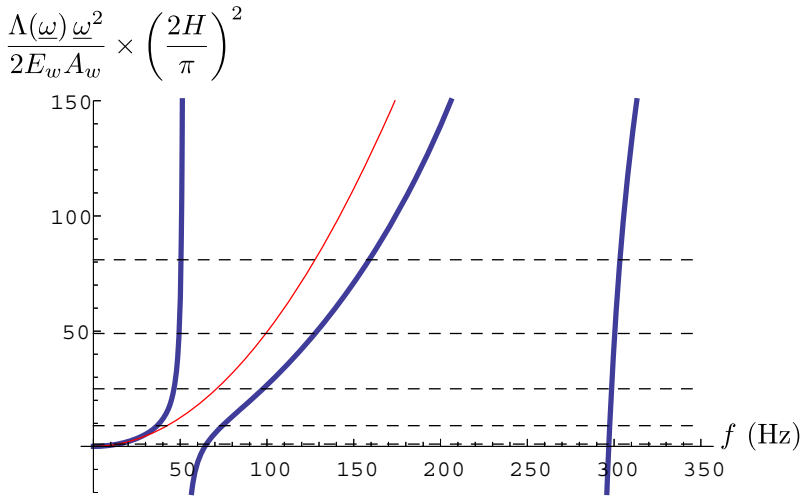

Figure 4.1. The thin red line is obtained by replacing the effective mass by the real mass. The thick blue line takes into account the resonance of the floors. The horizontal dashed lines indicate the first values of $(2k - 1)^2$. The resonance frequencies of the structure are the abscissas of the intersections of the continuous curves with the dashed lines.

Table 4.1. Comparison of the resonance frequencies (Hz) of the structure estimated thanks to the homogenized models and with the finite element code CESAR-LCPC.

k	Resonance of the floors neglected (Eqn. 3.2a)	Resonance of the floors taken into account (Eqn. 4.3.)	CESAR-LCPC with Euler-Bernoulli beams	CESAR-LCPC with Timoshenko beams
1	14.19	14.00 - 65.14 - 297.0	13.76 - 64.83	13.73 - 61.35
2	42.56	36.73 - 74.35 - 297.5	35.99 - 74.22	35.12 - 71.71
3	70.94	46.42 - 97.68 - 298.5	45.46 - 97.37	43.32 - 96.04
4	99.31	49.36 - 127.8 - 300.4	48.28 - 127.0	45.66 - 125.5
5	127.69	50.49 - 158.9 - 303.4	49.76 - 157.5	46.93 - 154.2

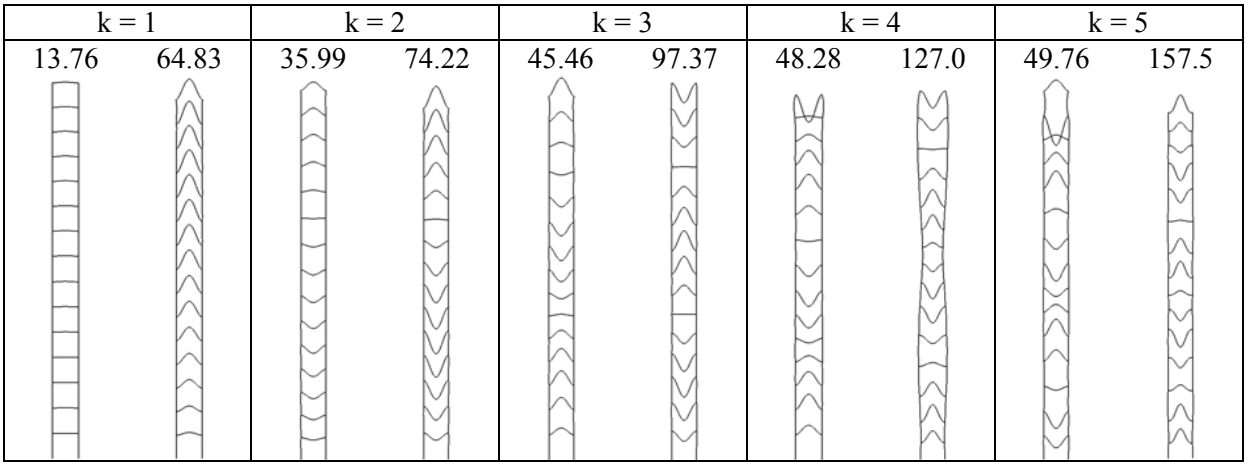

Figure 4.2. Modal shapes and resonance frequencies calculated with the finite element code CESAR-LCPC

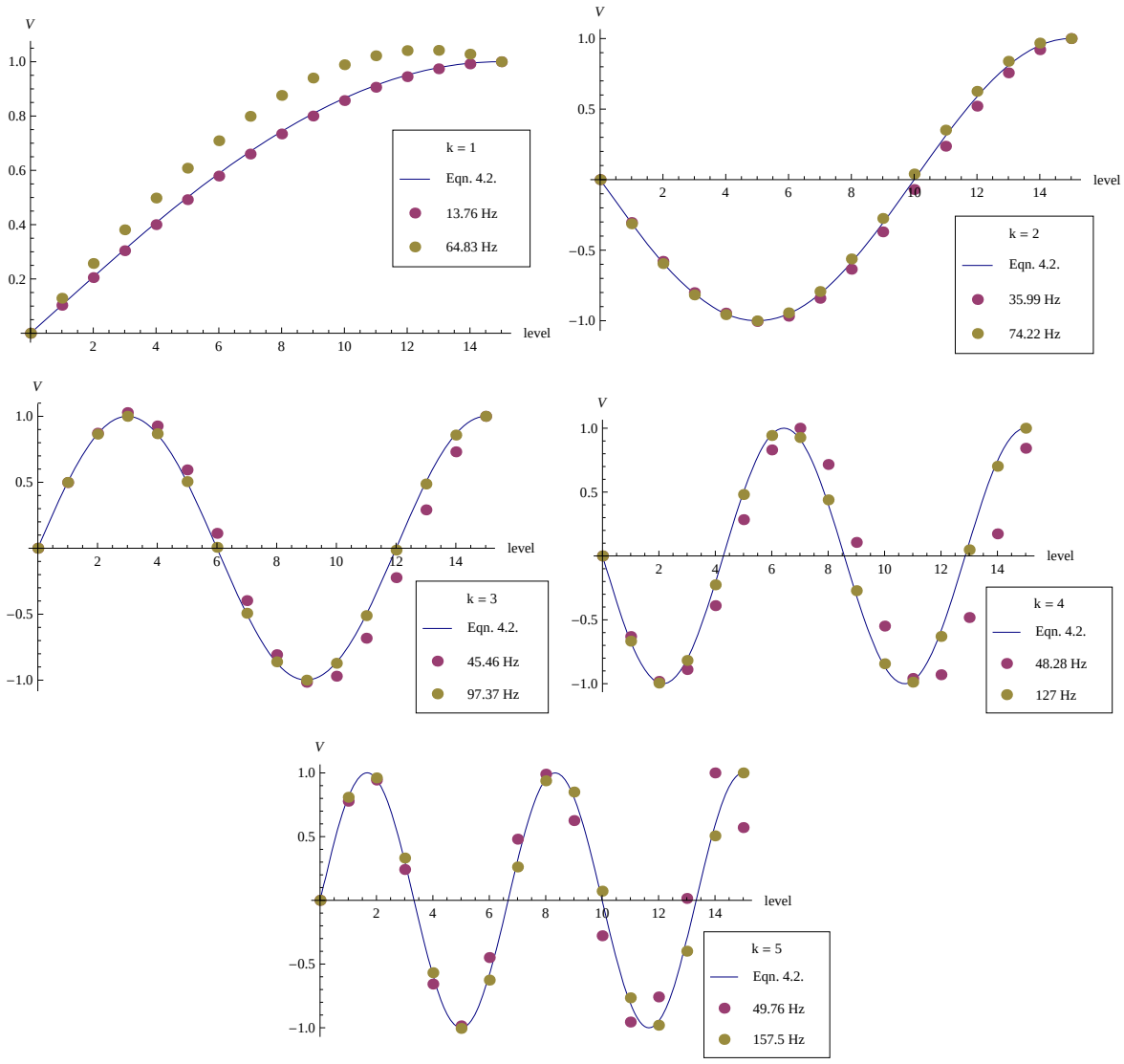

Figure 4.3. Comparison of the vertical displacements estimated with the homogenized model (Eqn. 4.2.) and the finite element code CESAR-LCPC

4.2. Harmonic motion at the bottom

A harmonic vertical motion of amplitude V_0 is now imposed at the bottom of the structure. We are interested in the evolution with the frequency of the amplitude of the displacement at the top. The solution of the homogenized model (Eqn. 3.5a) depends on the sign of the effective mass as indicated in Eqn. 4.4.

$$\Lambda(\underline{\omega}) \geq 0 \quad \Rightarrow \quad V(x) = V_0\left[\cos(\alpha\, x) + \tan(\alpha\, H)\sin(\alpha\, x)\right] \quad \Rightarrow \quad H(\underline{\omega}) = \frac{V(H)}{V_0} = \frac{1}{\cos(\alpha\, H)} \tag{4.4a}$$

$$\Lambda(\underline{\omega}) < 0 \quad \Rightarrow \quad V(x) = V_0\left[\cosh(\alpha\, x) - \tanh(\alpha\, H)\sinh(\alpha\, x)\right] \quad \Rightarrow \quad H(\underline{\omega}) = \frac{1}{\cosh(\alpha\, H)} \tag{4.4b}$$

$$\text{with } \alpha^2 = \frac{\left|\Lambda(\underline{\omega})\right|\underline{\omega}^2}{2\, E_w\, A_w}$$

The variations of the transfer function $H(\underline{\omega})$ according to the frequency are plotted in Fig. 4.4. As expected, there are peaks at the natural frequencies of the structure determined in section 4.1. Just before the first resonance of the floors at 52 Hz, the peaks are very numerous because of the great variations of the effective mass. However, a lot of them does not correspond to real modes of the structure. The homogenization process replaces the structure by an equivalent beam which has an infinite number of degrees of freedom and therefore a infinite number of vertical modes. On the contrary, the studied structure has only 15 possible macroscopic modal shapes. Just after the resonance of the floors, the effective mass is negative and we observe a bandgap, that is to say a frequency range with no motion at the top of the structure.

All these results are confirmed numerically. The transfer function computed with the finite element method is almost identical (Fig. 4.4.). As explained above, there are less peaks before the resonance of the floors and the bandgap begins at slightly lower frequencies. An example of the deformation of the structure inside the bandgap is also presented in Fig. 4.4. The first floors experience large deformations because of the resonance but the energy is not transferred to the upper storeys. From the fourth floor, there is no more vibration.

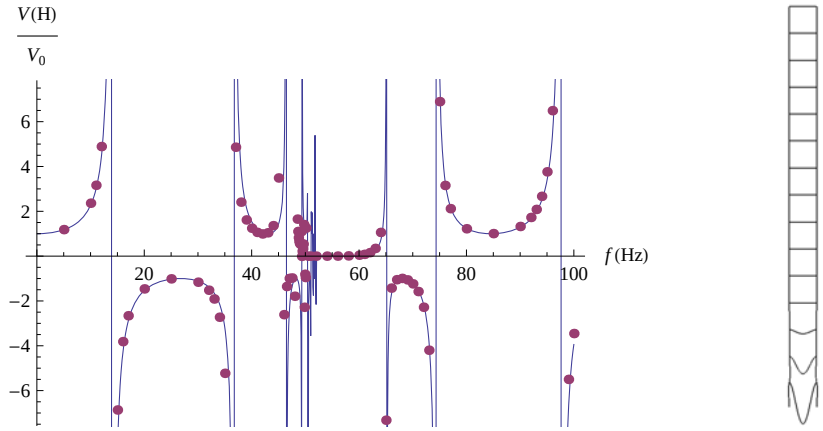

Figure 4.4. Left: transfer function of the studied structure. The continuous curve corresponds to the homogenized model (Eqn.4.4.) and the points to finite elements simulations. Right: deformation at 52 Hz.

The introduction of damping does not modify fundamentally the results. We use a complex elastic modulus $E_f = E_w = E\ e^{i\eta}$ in the homogenized model (Eqn. 4.4.). The modulus of the transfer function is plotted in Fig. 4.5. for $\eta = 2.10^{-2}$. The main difference with Fig. 4.4. is that the frequency bandgap is larger. As a result, the peaks of the transfer function before the resonance no longer exist.

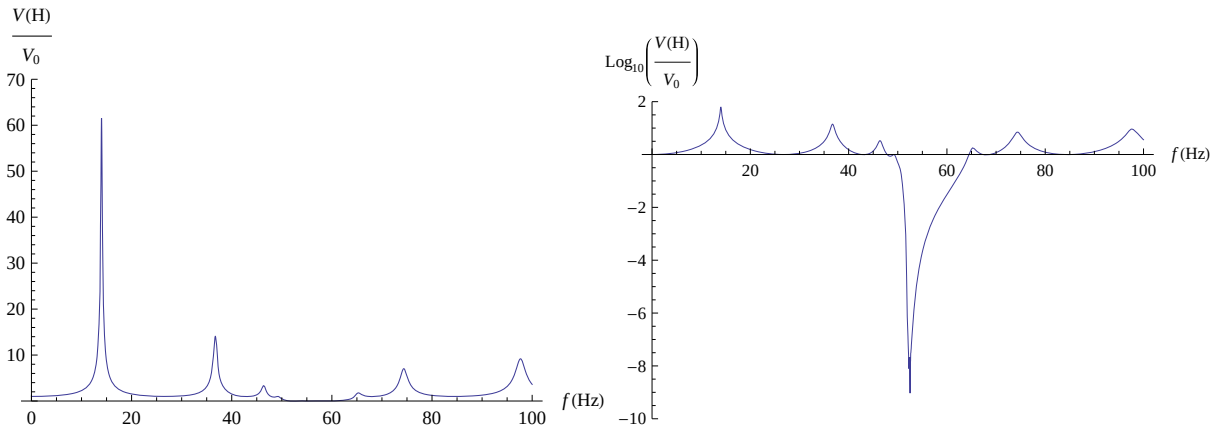

Figure 4.5. Modulus of the transfer function of the studied structure with damping.

5. CONCLUSION

Because of the rigidity contrast between tension-compression and bending in the beams and plates that constitute buildings, the vertical modes of a structure can appear in the same frequency range as the bending modes of the floors. The extension of the HPDM method to these situations with local resonance shows that the real mass should be replaced by an effective mass which depends on the frequency. When the frequency approaches the odd natural frequencies of the floors in bending, the effective mass becomes infinite and it changes its sign. This phenomenon has two main consequences. First, several normal modes of the structure associated to different natural frequencies can have the same macroscopic modal shapes. Second, when the effective mass is negative, the vibrations do not propagate inside the structure and we have frequency bandgaps.

These theoretical results are confirmed by finite elements simulations. The studied structure has been specially designed to highlight the effects of the local resonance. In particular, mass has been added to the floors. The increase of the length of the floors would have been another possibility. In real structures, the proportion of the mass affected by the resonance is probably smaller. In that case, the variations of the effective mass far from the resonance frequencies can be negligible. However, at the resonance, the effective mass is still considerable and the vibrations are attenuated.

REFERENCES

Auriault, J-L. and Bonnet, G. (1985). Dynamique des composites élastiques périodiques. *Achives of Mechanics*. **37:4-5**, 269-284.

Boutin, C. and Hans, S. (2003). Homogenisation of periodic discrete medium: Application to dynamics of framed structures. *Computers and Geotechnics*. **30:4**, 303-320.

Caillerie, D., Trompette, P. and Verna, P**.** (1989). Homogenisation of periodic trusses. *IASS Symposium, 10 Years of progress in Shell and Spatial Structures*.

Chesnais, C., Boutin, C. and Hans, S. (2011). Structural Dynamics and Generalized Continua. *In Mechanics of Generalized Continua*, Advanced Structured Materials, Springer, 57-76.

Hans, S. and Boutin, C. (2008). Dynamics of discrete framed structures: A unified homogenized description. *Journal of Mechanics of Materials and Structure.s* **3:9**, 1709-1739.

Hans, S., Boutin, C., Chesnais, C., Rallu, A. and Bui, Q. B. (2012). From ambient mechanical noise to the structural functioning of regular buildings. *15th World Conference on Earthquake Engineering.* **1530**.

Liu, Z., Zhang, X. X., Mao, Y. W., Zhu, Y. Y., Yang, Z. Y., Chan, C. T. and Sheng, P. (2000). Locally resonant sonic materials. *Science.* **289:5485**, 1734-1736.

Milton, G. W. and Willis, J. R. (2007). On modifications of Newton's second law and linear continuum elastodynamics. *Proceedings of the Royal Society A.* **463:2079**, 855-880.

Tollenaere, H., and Caillerie, D. (1998). Continuous Modeling of lattice structures by homogenization. *Advances in Engineering Software.* **29:7-9**, 699-705.